Neuroscience 293 (2015) 157–170

PROTEOMIC ANALYSES REVEAL THAT LOSS OF TDP-43 AFFECTS RNA PROCESSING AND INTRACELLULAR TRANSPORT

M. ŠTALEKAR,[a,c] X. YIN,[b] K. REBOLJ,[a] S. DAROVIC,[a,c] C. TROAKES,[c] M. MAYR,[b] C. E. SHAW[c] AND B. ROGELJ[a,d]*

[a] *Department of Biotechnology, Jožef Stefan Institute, Jamova 39, SI-1000 Ljubljana, Slovenia*

[b] *Cardiovascular Division, King's College London BHF Centre, 125 Coldharbour Lane, London SE5 9NU, United Kingdom*

[c] *Department of Clinical Neuroscience, Institute of Psychiatry, King's College London, 1 Windsor Walk, London SE5 8AF, United Kingdom*

[d] *Biomedical Research Institute BRIS, Puhova 10, SI-1000 Ljubljana, Slovenia*

Abstract—Transactive response DNA-binding protein 43 (TDP-43) is a predominantly nuclear, ubiquitously expressed RNA and DNA-binding protein. It recognizes and binds to UG repeats and is involved in pre-mRNA splicing, mRNA stability and microRNA metabolism. TDP-43 is essential in early embryonic development but accumulates in cytoplasmic aggregates in amyotrophic lateral sclerosis (ALS) and tau-negative frontotemporal lobar degeneration (FTLD). It is not known yet whether cytoplasmic aggregates of TDP-43 are toxic or protective but they are often associated with a loss of TDP-43 from the nucleus and neurodegeneration may be caused by a loss of normal TDP-43 function or a gain of toxic function. Here we present a proteomic study to analyze the effect of loss of TDP-43 on the proteome. MS data are available via ProteomeXchange with identifier PXD001668. Our results indicate that TDP-43 is an important regulator of RNA metabolism and intracellular transport. We show that Ran-binding protein 1 (RanBP1), DNA methyltransferase 3 alpha (Dnmt3a) and chromogranin B (CgB) are downregulated upon TDP-43 knockdown. Subsequently, transportin 1 level is increased as a result of RanBP1 depletion. Improper regulation of these proteins and the subsequent disruption of cellular processes may play a role in the pathogenesis of the TDP-43 proteinopathies ALS and FTLD.

Key words: TDP-43, RanBP1, amyotrophic lateral sclerosis, frontotemporal lobar degeneration, comparative proteomics, intracellular transport.

INTRODUCTION

The ubiquitously expressed RNA- and DNA-binding protein 43 (TDP-43) has attracted much scientific attention since it was identified as the major component of ubiquitinated cytoplasmic inclusions that are the pathological hallmark of amyotrophic lateral sclerosis (ALS) and frontotemporal lobar degeneration (FTLD), two devastating and incurable neurodegenerative disorders (Arai et al., 2006; Neumann et al., 2006). As a DNA-binding protein, it acts as a transcriptional repressor (Ou et al., 1995; Acharya et al., 2006), but even more important is its RNA-binding activity, through which it regulates RNA metabolism. By binding to preferentially UG-rich RNA sequences, it is involved in splicing regulation (Buratti and Baralle, 2001; Polymenidou et al., 2011; Tollervey et al., 2011). Furthermore, it regulates mRNA stability (Volkening et al., 2009) and microRNA biogenesis (Buratti et al., 2010).

TDP-43 is a predominantly nuclear RNA-binding protein but is known to shuttle between the nucleus and the cytoplasm (Nishimura et al., 2010) where it is sequestered to stress granules in response to oxidative stress (Colombrita et al., 2009). Similarly, TDP-43 accumulates in the cytoplasm, predominantly in the neurons that degenerate in ALS and FTLD, forming ubiquitinated hyperphosphorylated insoluble inclusions (Neumann et al., 2006). These cytoplasmic aggregates are often accompanied by clearance of TDP-43 from the nucleus implicating a sequestration of TDP-43, potentially causing a loss of function in the nuclear and cytoplasmic compartments.

We and others have identified many mutations in the gene encoding TDP-43 in familial and sporadic ALS which account for 1–5% of all ALS cases (Gitcho et al., 2008; Kabashi et al., 2008; Rutherford et al., 2008; Sreedharan et al., 2008; Van Deerlin et al., 2008; Yokoseki et al., 2008).

The molecular mechanism of the disease is still poorly understood and it is unclear whether TDP-43 inclusions are harmful to neurons via toxic gain of function or loss of function. Overexpression of mutant human TDP-43 in zebrafish caused motor neuron defects, wild-type TDP-43 less. Knockdown of zebrafish tardbp led to a similar phenotype (Kabashi et al., 2010). Overexpression of mutant human TDP-43 in mice and rats leads to neurodegeneration but TDP-43 inclusions are not always present (Wegorzewska et al., 2009; Zhou et al., 2010; Gendron and Petrucelli, 2011; Swarup et al., 2011; Tsao et al., 2012; Liu et al., 2013). On the contrary, rats and mice overexpressing wild-type human TDP-43 are not affected

*Correspondence to: B. Rogelj, Department of Biotechnology, Jožef Stefan Institute, Jamova 39, SI-1000 Ljubljana, Slovenia. Tel: +386-1-477-3611.

E-mail address: boris.rogelj@ijs.si (B. Rogelj).

Abbreviations: ALS, amyotrophic lateral sclerosis; CgB, chromogranin B; Dnmt3a, DNA methyltransferase 3 alpha; FTLD, frontotemporal lobar degeneration; FUS, fused in sarcoma; RanBP1, Ran-binding protein 1; TDP-43, transactive response DNA-binding protein 43.

http://dx.doi.org/10.1016/j.neuroscience.2015.02.046
0306-4522/

(Zhou et al., 2010; Swarup et al., 2011). TDP-43 is essential in embryonic development as homozygous TDP-43 knockout mice are lethal at embryonic day 7.5, while heterozygous mice lacking TDP-43 exhibit decreased grip strength without evidence of motor neuron degeneration (Kraemer et al., 2010). Remarkably, conditional knockout mice lacking TDP-43 in motor neurons (Wu et al., 2012; Iguchi et al., 2013) and RNAi transgenic mice with loss of TDP-43 (Yang et al., 2014) exhibit age-dependent progressive motor neuron degeneration. Null mutations in the *Drosophila* orthologue of TDP-43 cause locomotion defects (Chang et al., 2014; Diaper et al., 2013a,b) and knockout in zebrafish leads to muscle degeneration, vascular dysfunction and reduced motor neuron axon outgrowth (Schmid et al., 2013). These knockout animal models with symptoms resembling ALS provide evidence for the loss of TDP-43 function theory.

In order to study the effect of TDP-43 depletion on gene expression, several groups used a microarray approach to map transcriptional changes, whether on cell lines (Ayala et al., 2008; Fiesel et al., 2010; Bose et al., 2011; Tollervey et al., 2011; Shiga et al., 2012; Yu et al., 2012; Park et al., 2013; Honda et al., 2014) or animal models (Hazelett et al., 2012), or RNA-seq (Polymenidou et al., 2011). Here we present the effect of TDP-43 depletion at the level of the proteome.

EXPERIMENTAL PROCEDURES

Cell culture and RNAi

SH-SY5Y cells were grown in DMEM/F12 (Gibco) supplemented with 10% FBS (Gibco) and pen-strep (Lonza, Basel, Switzerland). siRNA transfection was mediated by PepMute Plus (SignaGen Laboratories, Rockville, Maryland, USA), using 5 nM siRNA. Prior to siRNA transfection, growth medium was replaced by OptiMEM (Gibco, Life Technologies) with 10% FBS and pen-strep. siRNAs targeting TDP-43 were from Invitrogen (Stealth) and Ran-binding protein 1 (RanBP1) siRNA was from (Qiagen, Venlo, Netherlands) (FlexiTube). Cells were harvested 96 h post transfection.

Cell fractionation

Cells were grown in 6-cm Petri dishes. They were harvested in cold CLB buffer [50 mM Tris, pH 7.4, 10 mM NaCl, 0.5% Igepal Ca-630 (Sigma–Aldrich, St. Louis, Missouri, USA), 0.25% Triton X-100] and centrifuged for 5 min at 3000× *g*, 4 °C. Supernatant was transferred to a fresh tube and recentrifuged at 16,100× *g*, 4 °C for 10 min and the later supernatant was used as the cytoplasmic fraction.

The first pellet was washed three times in cold CLB and then resuspended in 1 × SDS loading buffer without bromophenol blue [62.5 mM Tris, pH 6.8, 10% glycerol, 2% SDS], sonicated, boiled for 5 min and recentrifuged. Supernatant was saved as the nuclear fraction. Protein concentration in fractions was determined using Bio-Rad DC Protein Assay.

Gel-LC–MS/MS

A method, described elsewhere (Yin et al., 2010), was used with some modifications. Samples were denatured with 2× sample loading buffer (Invitrogen, Life Technologies) at 96 °C for 5 min and then separated in 4–12% Bis-Tris polyacrylamide gels (Invitrogen) until the blue dye front reached the bottom of the gel. After SDS-PAGE, gels were stained using the Colloidal Blue Staining Kit (Invitrogen). The entire gel lane was excised and no ''empty'' gel pieces were left behind. Tryptic in-gel digestion was performed using the Investigator ProGest (Genomic Solutions) robotic digestion system with sequencing grade-modified trypsin (Promega, Madison, Wisconsin, USA) (Shevchenko et al., 1996; Wilm et al., 1996; Yin et al., 2010). Following enzymatic degradation, samples were separated by nano flow liquid chromatography on a reverse-phase column (C18 PepMap100, 3 μm, 100 Å, 25 cm; Thermo Fisher Scientific) using a 40-min gradient (2% A to 40% B where A is 2% ACN, 0.1% FA in HPLC H_2O and B is 90% ACN, 0.1% FA in HPLC H_2O) and applied to an LTQ Orbitrap XL mass spectrometer (Thermo Fisher Scientific, Waltham, Massachusetts, USA). Spectra were collected from the mass analyzer using a full ion scan mode over the m/z range 450–1600. For each full scan, MS/MS scans were performed on six most abundant ions using dynamic exclusion. The mass spectrometry proteomics data have been deposited to the ProteomeXchange Consortium (http://proteomecentral.proteomexchange.org) via the PRIDE partner repository (Vizcaino et al., 2014) with the dataset identifier PXD001668 and DOI 10.6019/PXD001668.

Protein identification

The MS/MS data were matched to UniProt/SwissProt human database (release version 57.15, 20,266 protein entries) using Mascot (version 2.3.01, Matrix Sciences). Carboxyamidomethylation of cysteine was used as a fixed modification, and oxidation of methionine was used as a variable modification. The mass tolerance was set at 10 ppm for the precursor ions and at 0.8 Da for fragment ions. Two missed cleavages were allowed. The search results were loaded into Scaffold software (version 3.3.1, Proteome Software) and protein and peptide probabilities were calculated. Assignments were accepted with > 99.0% protein probability, > 95.0% peptide probability, and a minimum of two peptides (Keller et al., 2002; Nesvizhskii et al., 2003).

Bioinformatics

Identified differentially expressed proteins were functionally annotated using DAVID Bioinformatics Resources 6.7 (Huang da et al., 2009a,b). *Homo sapiens* whole genome was used as background.

Immunoblotting

Reducing SDS-PAGE was run on 10% polyacrylamide gels loaded with 5 μg of protein samples in 1 × SDS loading buffer with 100 mM dithiothreitol at 150 V. Then, wet transfer to the nitrocellulose membrane was carried out at

200 mA for 90 min. Membranes were blocked in 5% non-fat dry milk in TBS-Tween (TBST) for 1 h at room temperature. Primary antibodies diluted in blocking medium were incubated for 1–4 h at room temperature. Membranes were washed three times with TBST and incubated with secondary HRPO-conjugated anti-rabbit (Jackson Immunoresearch, Newmarket, Suffolk, UK, 1:10,000) or anti-mouse (Millipore, Billerica, Massachusetts, USA, 1:10,000) diluted in blocking medium for 1 h at room temperature. After washing with TBST and TBS, chemiluminescent reagent (Luminol, Santa Cruz, Dallas, Texas, USA or Lumi-Light, Roche, Basel, Switzerland) was added and membranes were exposed to Amersham films. Films were developed using Kodak reagents and scanned. ImageJ software was used to relatively quantify protein bands.

Antibodies

Antibodies used are listed in Table 1.

Immunofluorescence

Cells were grown on glass cover slips (thickness number 1) and were fixed with 4% paraformaldehyde in PBS for 15 min or with methanol for 10 min at −20 °C. Paraformaldehyde-fixed cells were permeabilized with 0.1% Triton X-100 for 6 min. After washing with PBS, blocking was carried out with 3% BSA in PBS. Antibodies and TO-PRO-3 iodide (Invitrogen, 1:400) diluted in blocking medium were incubated for 1 h at room temperature. Cover slips were mounted with ProLong Gold antifade reagent (Invitrogen). Images were acquired using a Zeiss LSM 710 inverted confocal laser scanning microscope and ZEN 2010 B SP1 software. ImageJ was used to quantify immunofluorescence signal intensities.

Calculations and statistical analysis

Fisher's exact test using total spectrum counts of identified peptides from control and three TDP-43-knockdown replicates was performed to evaluate statistical significance of differential expression of proteins using the same parameters as for protein identification (i.e. >95.0% peptide probability and minimum of two peptides). $p < 0.05$ was regarded as statistically significant. Fold change was calculated as a ratio of average of total spectrum counts of a protein in TDP-43-knockdown samples to average of total spectrum counts of a protein in controls.

Quantitative values of protein bands in western blot were normalized to GAPDH in cytoplasmic fractions and fibrillarin in nuclear fractions and relative protein expression levels toward control were calculated. Regarding immunofluorescence images, immunofluorescence signal intensities of cells with silenced and normal TDP-43-expression in TDP-43 siRNA treatment were compared and relative protein expression levels were calculated. Statistical significance of differential expression of proteins according to western blot and immunofluorescence was evaluated with Student's *t*-test analysis. A *p*-value of <0.05 was considered significant.

Table 1. List of antibodies used in this study. Dilutions for western blot (WB) and immunofluorescence (IF) are presented

Target	Source	WB	IF
TDP-43	Proteintech, 10782-2-AP	1:6000	1:400
TDP-43	Millipore, MABN150		1:200
RanBP1	Abcam, ab2937	1:1000	1:1000
RanBP1	Novus Biologicals, NB100-79814	1:1000	
Dnmt3a	Santa Cruz, sc-20703	1:1500	1:100
HuD	Santa Cruz, sc-28299	1:500	1:50
GAPDH	Invitrogen, 39-8600	1:10,000	
fibrillarin	Santa Cruz, sc-25397	1:500	
EIF4G2	Santa Cruz, sc-135999	1:200	
CgB	Santa Cruz, sc-20135	1:200	
HSPB1	Santa Cruz, sc-13132	1:200	
MetRS	Santa Cruz, sc-98558	1:200	
LIS1	Santa Cruz, sc-15319	1:500	
transportin 1	Abcam, ab10303		1:100
TFRC	Santa Cruz, sc-32272	1:50	
LMNB1	Santa Cruz, sc-20682	1:20,000	

RESULTS

TDP-43 knockdown

We have used knockdown of TDP-43 in order to analyze the loss of its function on the total proteome of human neuroblastoma SH-SY5Y cells. We prepared nuclear and cytoplasmic fractions. All three TDP-43-targeting siRNAs used were efficient in silencing TDP-43. Western blots confirmed that we achieved 92.3 ± 0.5% knockdown of TDP-43 protein levels with siRNA 1 (8% expression relative to control) measured in nuclear fractions. We achieved a knockdown of 88.5 ± 0.2% with siRNA 2 and 62.1 ± 4.1% using siRNA 3 in nuclear fractions (Figs. 1A, C and 2) and decided to use siRNA 1 thereafter for silencing TDP-43 in this proteomic study.

Identification of differentially expressed proteins with comparative proteomics

Cells were harvested 96 h post transfection with either TDP-43 siRNA 1 or control siRNA. Cytoplasmic and nuclear fractions were separated on SDS–PAGE, each lane was divided into eight sections and analyzed by mass spectrometry. Six hundred and two proteins were identified in nuclear fractions and 949 proteins in cytoplasmic fractions. We then compared spectrum counts of peptides for each protein in control fractions and fractions of TDP-43-silenced cells. One hundred and six differentially abundant candidate proteins were identified in nuclear fractions ($p < 0.05$), 50 of them being decreased and 56 increased (Table 2). In cytoplasmic fractions, 167 proteins were differentially expressed of which 94 were decreased and 73 were increased (Table 3). Interestingly, the differentially expressed proteins from both fractions represent 17.6% of the proteins detected in the fraction. According to DAVID functional annotation, most of the differentially expressed proteins affect RNA processing and intracellular transport (Table 4).

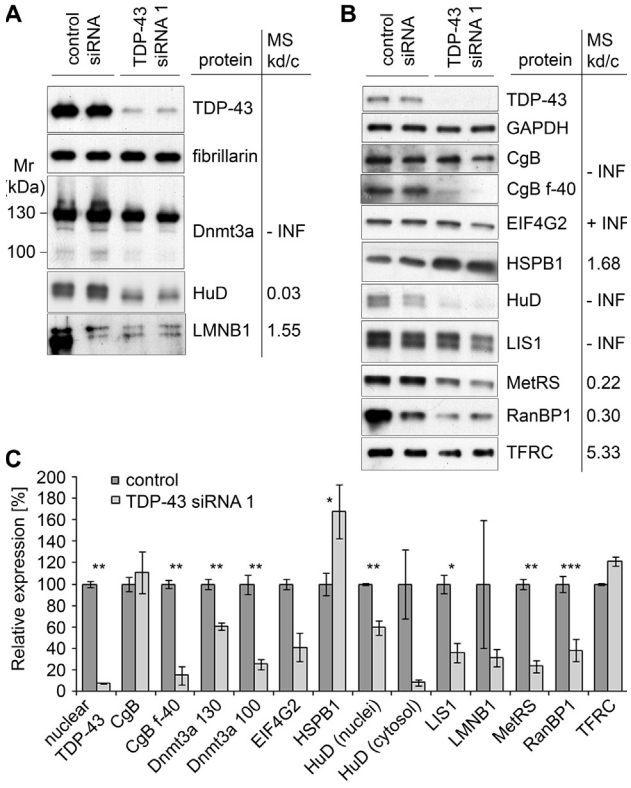

Fig. 1. Validation of mass spectrometry results with western blot. SH-SY5Y were transfected either with TDP-43 siRNA 1 or control siRNA. Cells were harvested 96 h later and nuclear (A) and cytoplasmic (B) fractions were analyzed by western blot. GAPDH and fibrillarin were used as loading controls for cytoplasmic and nuclear fractions, respectively. Knockdown vs. control ratios for the chosen proteins obtained from mass spectrometry data are presented in the table. +/− INF marks that protein was detected only in knockdown/control fractions. Panel C shows relative protein expression levels calculated from western blots. Seven proteins – CgB fragment, Dnmt3a, HSPB1, HuD, LIS1, MetRS and RanBP1 – are downregulated when cells are transfected with TDP-43 siRNA 1. Asterisks mark statistical significance: $^{*}p < 0.05$, $^{**}p < 0.01$ and $^{***}p < 0.001$.

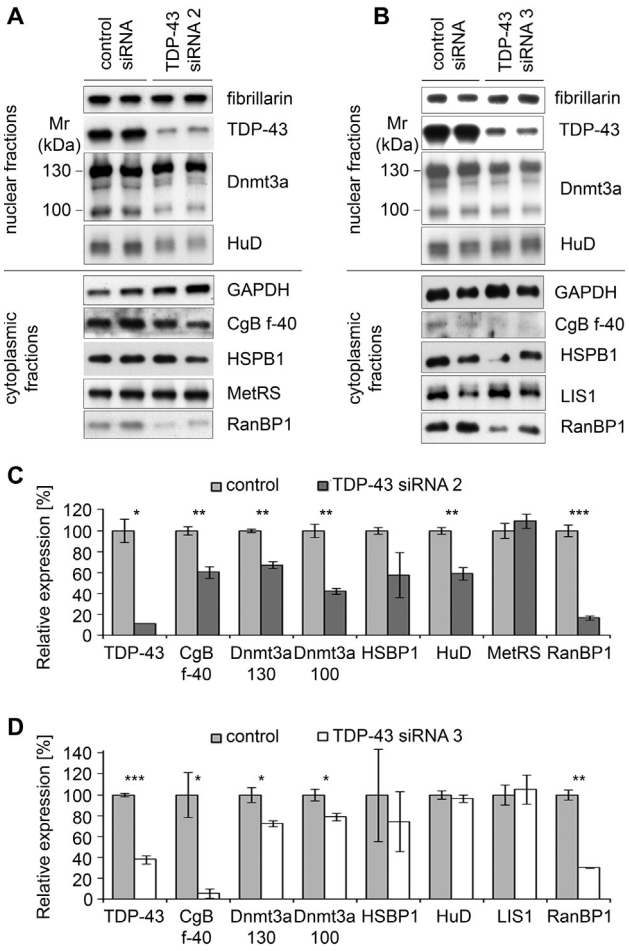

Fig. 2. Confirmation of TDP-43-specific targets with knockdown using different siRNAs. SH-SY5Y were transfected either with control, TDP-43 siRNA 2 (A and C) or 3 (B and D). 96 h later, subcellular fractions were prepared. Western blots (A, B) were probed for validated proteins from proteomic study and protein expression levels relative to control were calculated (C, D). We confirmed that TDP-43 positively regulates expression of a 40-kDa fragment of CgB, Dnmt3a and RanBP1. GAPDH and fibrillarin were used as loading controls for cytoplasmic and nuclear fractions, respectively. MetRS and LIS1 were probed with only one validation siRNA treatment as there was no significant change in their expression. Asterisks mark statistical significance: $^{*}p < 0.05$, $^{**}p < 0.01$ and $^{***}p < 0.001$.

Validation

To validate proteomic results, we chose 10 proteins and examined their expression levels in the SH-SY5Y cell line using western blot. The proteins were chosen based on the *p*-value of differential expression, literature information, function and commercial availability of the antibodies. With relative quantification of changes in the intensity of protein bands, we assessed our proteomic results to be 70% accurate as seven out of 10 tested proteins, namely CgB f-40 (a 40-kDa fragment of chromogranin B), DNA methyltransferase 3 alpha (Dnmt3a), HSPB1, HuD, LIS1, MetRS and RanBP1 (UniProt identifiers SCG1, DNM3A, HSPB1, ELAVL4, LIS1, SYMC and RANG, respectively – see Tables 2 and 3), showed the predicted differential expression with $p < 0.05$ (Fig. 1).

To rule out possible side effects or unspecific targeting of siRNA used in the proteomic study, we analyzed the expression of selected proteins in cells treated with siRNA 2 or siRNA 3. We confirmed downregulation of RanBP1, Dnmt3a and CgB f-40 when TDP-43 is depleted (Fig. 2).

We then performed immunofluorescence on SH-SY5Y cells 96 h after siRNA transfection and indeed we observed reduced levels of RanBP1 staining in the cytoplasm and Dnmt3a staining in nuclei of TDP-43-depleted cells (Fig. 3).

TNPO1 protein level is raised in SH-SY5Y cells with depleted RanBP1

Since RanBP1 is known to be involved in Ran-mediated nucleocytoplasmic transport (Bischoff et al., 1995), we were interested to examine whether its depletion arrests TDP-43 transport. We performed siRNA-mediated knockdown of RanBP1 in SH-SY5Y and achieved 98.5 ± 0.6% silencing after 96 h. RanBP1 depletion did not affect TDP-

Table 2. List of significantly changed proteins in the nuclear fraction following TDP-43 knockdown. Proteins are listed in order of significance (*p*-value obtained from Fisher's exact test). T/C ratio represents the protein ratio between TDP-43 knockdown (T) and control (C). C1N-C3N and T1N-T3N represent total spectra counts for identified proteins from triplicate control (C) and TDP-43(T) quantifications

Protein name	UniProtKB/Swiss-Prot identifier	*p*-value	T/C ratio	Total spectra					
				C1N	C2N	C3N	T1N	T2N	T3N
Histone H2B-type 1-B	H2B1B_HUMAN	< 0.00010	−INF	0	18	19	0	0	0
Sister chromatid cohesion protein PDS5 homolog B	PDS5B_HUMAN	< 0.00010	−INF	2	7	5	0	0	0
ELAV-like protein 4	ELAV4_HUMAN	< 0.00010	0.03	23	19	17	0	2	0
Hexokinase-1	HXK1_HUMAN	< 0.00010	0.14	6	6	10	0	3	0
Antigen KI-67	KI67_HUMAN	< 0.00010	0.33	18	22	11	3	8	6
Keratin, type I cytoskeletal 10	K1C10_HUMAN	< 0.00010	2.46	17	15	3	30	38	18
Actin, alpha cardiac muscle 1	ACTC_HUMAN	< 0.00010	3.47	0	0	30	32	31	41
ATP-dependent DNA helicase 2 subunit 2	KU86_HUMAN	< 0.00010	+INF	0	0	0	5	8	4
Lamin-B2	LMNB2_HUMAN	< 0.00010	+INF	0	0	0	10	8	9
Heterogeneous nuclear ribonucleoprotein H3	HNRH3_HUMAN	0.00018	7.00	3	0	0	8	8	5
RNA-binding protein 28	RBM28_HUMAN	0.00022	5.00	2	3	0	7	11	7
Pinin	PININ_HUMAN	0.00029	+INF	0	0	0	3	6	3
Nestin	NEST_HUMAN	0.00047	0.72	78	66	64	58	52	40
mRNA turnover protein 4 homolog	MRT4_HUMAN	0.00057	+INF	0	0	0	6	3	2
Replication factor C subunit 4	RFC4_HUMAN	0.00057	+INF	0	0	0	4	5	2
Tubulin beta-2B chain	TBB2B_HUMAN	0.00075	2.92	0	0	12	13	10	12
T-complex protein 1 subunit eta	TCPH_HUMAN	0.00084	−INF	3	3	4	0	0	0
Torsin-1A-interacting protein 1	TOIP1_HUMAN	0.00084	−INF	3	3	4	0	0	0
Keratin, type I cytoskeletal 14	K1C14_HUMAN	0.0011	+INF	0	0	0	0	0	10
Periodic tryptophan protein 2 homolog	PWP2_HUMAN	0.0016	5.67	3	0	0	7	5	5
Guanine nucleotide-binding protein G(k) subunit alpha	GNAI3_HUMAN	0.0017	-INF	6	3	0	0	0	0
NADH dehydrogenase [ubiquinone] 1 beta subcomplex subunit 10	NDUBA_HUMAN	0.0017	-INF	3	3	3	0	0	0
DNA topoisomerase 2-alpha	TOP2A_HUMAN	0.0018	0.52	20	16	18	8	14	6
Nuclear pore complex protein Nup153	NU153_HUMAN	0.0022	+INF	0	0	0	5	2	2
Nucleolar RNA helicase 2	DDX21_HUMAN	0.0024	1.46	37	30	43	52	51	58
Nucleolar GTP-binding protein 1	NOG1_HUMAN	0.0033	2.80	0	5	5	10	9	9
Keratin, type II cuticular Hb5	KRT85_HUMAN	0.0035	−INF	8	0	0	0	0	0
T-complex protein 1 subunit zeta	TCPZ_HUMAN	0.0035	−INF	0	2	6	0	0	0
U3 small nucleolar ribonucleoprotein protein IMP3	IMP3_HUMAN	0.0035	−INF	2	2	4	0	0	0
Nuclear pore complex protein Nup205	NU205_HUMAN	0.0036	0.42	7	13	11	6	5	2
Lamin-B1	LMNB1_HUMAN	0.0036	1.55	22	24	27	35	44	34
Isochorismatase domain-containing protein 1	ISOC1_HUMAN	0.0038	2.89	0	6	3	8	8	10
60S ribosomal protein L27	RL27_HUMAN	0.0044	+INF	0	0	0	3	2	3
DNA-directed RNA polymerase I subunit RPA1	RPA1_HUMAN	0.0044	+INF	0	0	0	4	4	0
G patch domain-containing protein 4	GPTC4_HUMAN	0.0044	+INF	0	0	0	5	3	0
FACT complex subunit SSRP1	SSRP1_HUMAN	0.0049	0.25	10	3	3	0	2	2
Spectrin alpha chain, brain	SPTA2_HUMAN	0.0052	0.78	66	68	66	57	63	36
60S ribosomal protein L7	RL7_HUMAN	0.0066	2.88	0	4	4	9	7	7
Ribosomal RNA-processing protein 7 homolog A	RRP7A_HUMAN	0.0071	−INF	2	0	5	0	0	0
Pre-mRNA-splicing factor ISY1 homolog	ISY1_HUMAN	0.0075	6.00	0	2	0	3	4	5
ATP-binding cassette sub-family F member 1	ABCF1_HUMAN	0.0086	+INF	0	0	0	4	3	0
ATP-dependent RNA helicase DDX54	DDX54_HUMAN	0.0086	+INF	0	0	0	3	2	2
Midasin	MDN1_HUMAN	0.0086	+INF	0	0	0	4	3	0
mRNA export factor	RAE1L_HUMAN	0.0086	+INF	0	0	0	4	3	0
YLP motif-containing protein 1	YLPM1_HUMAN	0.0086	+INF	0	0	0	3	4	0
ATP synthase subunit beta, mitochondrial	ATPB_HUMAN	0.0091	0.23	0	0	13	0	0	3
Tyrosine-protein kinase Lyn	LYN_HUMAN	0.0091	0.23	6	3	4	0	3	0
ADP/ATP translocase 3	ADT3_HUMAN	0.011	0.46	17	0	11	0	0	13
Polymerase delta-interacting protein 3	PDIP3_HUMAN	0.012	2.86	0	4	3	9	4	7
Putative rRNA methyltransferase 3	RRMJ3_HUMAN	0.012	4.33	3	0	0	5	5	3
40S ribosomal protein S7	RS7_HUMAN	0.014	−INF	3	0	3	0	0	0
Keratin, type II cuticular Hb6	KRT86_HUMAN	0.014	−INF	6	0	0	0	0	0
Splicing factor 1	SF01_HUMAN	0.014	−INF	4	2	0	0	0	0
Structural maintenance of chromosomes protein 3	SMC3_HUMAN	0.014	0.58	13	15	15	11	14	0
Nuclear mitotic apparatus protein 1	NUMA1_HUMAN	0.014	0.82	74	73	62	66	72	33
Flap endonuclease 1	FEN1_HUMAN	0.015	0.25	4	3	5	3	0	0
Leucine-rich repeat-containing protein 59	LRC59_HUMAN	0.015	0.25	5	3	4	0	3	0

(*continued on next page*)

Table 2 (*continued*)

Protein name	UniProtKB/Swiss-Prot identifier	*p*-value	T/C ratio	Total spectra					
				C1N	C2N	C3N	T1N	T2N	T3N
Myosin-9	MYH9_HUMAN	0.015	0.83	76	75	74	70	77	39
28-kDa heat- and acid-stable phosphoprotein	HAP28_HUMAN	0.017	+INF	0	0	0	3	0	3
Cysteine and glycine-rich protein 2	CSRP2_HUMAN	0.017	+INF	0	0	0	6	0	0
Nuclear envelope pore membrane protein POM 121C	P121C_HUMAN	0.017	+INF	0	0	0	3	3	0
Protein mago nashi homolog 2	MGN2_HUMAN	0.017	+INF	0	0	0	0	3	3
Histone-binding protein RBBP4	RBBP4_HUMAN	0.018	1.74	9	11	7	15	17	15
60S ribosomal protein L11	RL11_HUMAN	0.018	3.50	4	0	0	4	4	6
Heterochromatin protein 1-binding protein 3	HP1B3_HUMAN	0.021	0.45	2	17	3	4	6	0
Probable ATP-dependent RNA helicase DDX17	DDX17_HUMAN	0.021	0.75	41	33	32	24	33	23
40S ribosomal protein S10	RS10_HUMAN	0.022	0.38	7	5	4	6	0	0
Paired amphipathic helix protein Sin3a	SIN3A_HUMAN	0.022	5.00	0	2	0	6	0	4
Heat shock protein HSP 90-beta	HS90B_HUMAN	0.023	0.57	8	3	24	3	3	14
Myb-binding protein 1A	MBB1A_HUMAN	0.023	1.46	21	21	17	25	39	22
Galectin-1	LEG1_HUMAN	0.027	0.41	6	5	6	0	7	0
U3 small nucleolar RNA-associated protein 15 homolog	UTP15_HUMAN	0.028	3.25	4	0	0	5	4	4
Cytochrome c	CYC_HUMAN	0.029	−INF	0	2	3	0	0	0
DNA (cytosine-5)-methyltransferase 3A	DNM3A_HUMAN	0.029	−INF	3	2	0	0	0	0
Heat shock protein HSP 90-alpha	HS90A_HUMAN	0.029	−INF	0	0	5	0	0	0
Probable dimethyladenosine transferase	DIMT1_HUMAN	0.029	−INF	0	2	3	0	0	0
Trifunctional enzyme subunit alpha, mitochondrial	ECHA_HUMAN	0.029	−INF	3	0	2	0	0	0
Voltage-dependent calcium channel subunit alpha-2/delta-1	CA2D1_HUMAN	0.029	−INF	2	3	0	0	0	0
WD repeat-containing protein 43	WDR43_HUMAN	0.029	−INF	0	2	3	0	0	0
Flotillin-2	FLOT2_HUMAN	0.031	0.64	13	18	14	10	9	10
Septin-9	SEPT9_HUMAN	0.032	1.56	7	8	21	20	20	16
ATP-dependent RNA helicase DDX3X	DDX3X_HUMAN	0.033	0.54	7	12	7	0	7	7
Heterogeneous nuclear ribonucleoprotein L	HNRPL_HUMAN	0.034	1.38	24	22	25	30	34	34
Pre-mRNA-processing factor 6	PRP6_HUMAN	0.034	1.79	7	6	6	10	14	10
AP-2 complex subunit mu	AP2M1_HUMAN	0.034	+INF	0	0	0	0	2	3
Mitochondrial carrier homolog 2	MTCH2_HUMAN	0.034	+INF	0	0	0	0	5	0
Nuclear pore complex protein Nup160	NU160_HUMAN	0.034	+INF	0	0	0	2	0	3
Single-stranded DNA-binding protein, mitochondrial	SSBP_HUMAN	0.034	+INF	0	0	0	0	5	0
U3 small nucleolar RNA-associated protein 14 homolog A	UT14A_HUMAN	0.034	+INF	0	0	0	0	2	3
U4/U6 small nuclear ribonucleoprotein Prp3	PRPF3_HUMAN	0.034	+INF	0	0	0	2	3	0
Microtubule-associated protein 1B	MAP1B_HUMAN	0.036	0.56	9	13	5	2	6	7
Protein RCC2	RCC2_HUMAN	0.036	2.80	3	2	0	2	9	3
60S ribosomal protein L23	RL23_HUMAN	0.036	4.50	0	2	0	3	6	0
Nucleolysin TIAR	TIAR_HUMAN	0.036	4.50	0	2	0	3	0	6
Ran GTPase-activating protein 1	RAGP1_HUMAN	0.036	4.50	2	0	0	4	5	0
Caldesmon	CALD1_HUMAN	0.039	1.41	24	16	19	30	28	25
Far upstream element-binding protein 2	FUBP2_HUMAN	0.04	1.42	18	21	16	25	24	29
Bystin	BYST_HUMAN	0.043	3.00	2	2	0	4	4	4
Treacle protein	TCOF_HUMAN	0.044	1.53	11	23	0	18	13	21
Keratin, type II cytoskeletal 2 epidermal	K22E_HUMAN	0.044	1.74	7	7	5	12	13	8
Histone H2B type 1-C/E/F/G/I	H2B1C_HUMAN	0.045	0.76	27	22	30	20	13	27
60 kDa heat shock protein, mitochondrial	CH60_HUMAN	0.046	0.47	4	5	8	3	3	2
Histone H3.1	H31_HUMAN	0.046	0.47	4	3	10	4	4	0
Transformation/transcription domain-associated protein	TRRAP_HUMAN	0.046	0.47	6	7	4	6	2	0
Chromobox protein homolog 3	CBX3_HUMAN	0.048	0.61	14	11	6	6	8	5
Guanine nucleotide-binding protein G(s) subunit alpha isoforms XLas	GNAS1_HUMAN	0.048	0.75	29	20	24	18	19	18

43 or Dnmt3a protein level as shown by western blot of cell lysates (Fig. 4C). We next compared the localisation of transportin 1 in cells with silenced RanBP1. We did not detect any significant difference in the distribution of transportin 1 between the nucleus and cytosol compared to controls. Instead, we noticed about 40% overall

Table 3. List of significantly changed proteins in the cytosolic fraction following TDP-43 knockdown. Proteins are listed in order of significance (*p*-value obtained from Fisher's exact test). T/C ratio represents the protein ratio between TDP-43 knockdown (T) and control (C). C1N-C3C and T1N-T3C represent total spectra counts for identified proteins from triplicate control (C) and TDP-43(T) quantifications

Protein name	UniProtKB/Swiss-Prot identifier	*p*-value	T/C ratio	Total spectra					
				C1C	C2C	C3C	T1C	T2C	T3C
Beta-actin-like protein 2	ACTBL_HUMAN	< 0.00010	−INF	12	0	10	0	0	0
ELAV-like protein 4	ELAV4_HUMAN	< 0.00010	−INF	5	5	5	0	0	0
Secretogranin-1	SCG1_HUMAN	< 0.00010	−INF	10	13	8	0	0	0
E3 ubiquitin-protein ligase HUWE1	HUWE1_HUMAN	< 0.00010	0.08	11	2	12	2	0	0
Dihydrolipoyl dehydrogenase, mitochondrial	DLDH_HUMAN	< 0.00010	0.10	11	9	10	3	0	0
Phosphoglycerate mutase 1	PGAM1_HUMAN	< 0.00010	0.17	15	12	14	0	0	7
Serine/arginine repetitive matrix protein 2	SRRM2_HUMAN	< 0.00010	0.22	11	14	7	3	4	0
Keratin, type I cytoskeletal 10	K1C10_HUMAN	< 0.00010	0.47	56	36	52	23	11	33
Keratin, type II cytoskeletal 1	K2C1_HUMAN	< 0.00010	0.64	80	67	78	57	35	51
Spectrin beta chain, brain 1	SPTB2_HUMAN	< 0.00010	0.65	84	35	87	58	25	51
Neuroblast differentiation-associated protein AHNAK	AHNK_HUMAN	< 0.00010	0.65	94	82	86	86	25	58
Microtubule-associated protein 1B	MAP1B_HUMAN	< 0.00010	0.68	118	110	104	89	61	76
Vimentin	VIME_HUMAN	< 0.00010	1.68	61	57	74	99	119	105
Tubulin beta-4 chain	TBB4_HUMAN	< 0.00010	2.70	40	0	0	34	39	35
Heat shock protein 75 kDa, mitochondrial	TRAP1_HUMAN	< 0.00010	5.20	0	5	0	8	9	9
Nucleoside diphosphate kinase B	NDKB_HUMAN	< 0.00010	+INF	0	0	0	0	11	10
Polyadenylate-binding protein 4	PABP4_HUMAN	< 0.00010	+INF	0	0	0	9	13	0
60S ribosomal protein L15	RL15_HUMAN	< 0.00010	+INF	0	0	0	4	4	8
28S ribosomal protein S29, mitochondrial	RT29_HUMAN	< 0.00010	+INF	0	0	0	6	5	4
Polyadenylate-binding protein 1	PABP1_HUMAN	0.00011	2.55	0	15	5	11	22	18
Superoxide dismutase [Mn], mitochondrial	SODM_HUMAN	0.00011	+INF	0	0	0	5	6	2
60S ribosomal protein L18	RL18_HUMAN	0.00012	7.00	0	0	3	5	6	10
Glutaredoxin-3	GLRX3_HUMAN	0.00022	+INF	0	0	0	2	5	5
Eukaryotic initiation factor 4A-III	IF4A3_HUMAN	0.00022	+INF	0	0	0	7	0	5
Filamin-B	FLNB_HUMAN	0.00023	1.53	36	32	35	61	41	56
Tubulin alpha-1B chain	TBA1B_HUMAN	0.00023	1.44	40	39	63	63	67	75
Transketolase	TKT_HUMAN	0.00023	2.69	9	3	4	12	17	14
14-3-3 protein gamma	1433G_HUMAN	0.00023	5.50	4	0	0	9	6	7
Stimulated by retinoic acid gene 6 protein homolog	STRA6_HUMAN	0.00027	−INF	5	3	4	0	0	0
Platelet-activating factor acetylhydrolase IB subunit alpha	LIS1_HUMAN	0.00053	−INF	4	4	3	0	0	0
Methionyl-tRNA synthetase, cytoplasmic	SYMC_HUMAN	0.00053	0.22	8	8	7	0	2	3
Calcium-binding mitochondrial carrier protein Aralar2	CMC2_HUMAN	0.00058	8.00	2	0	0	5	6	5
Spectrin alpha chain, brain	SPTA2_HUMAN	0.00071	0.74	108	91	96	91	49	78
60S ribosomal protein L3	RL3_HUMAN	0.00073	0.37	14	15	9	6	8	0
Endophilin-A2	SH3G1_HUMAN	0.0009	+INF	0	0	0	4	4	2
Cytoplasmic FMR1-interacting protein 1	CYFP1_HUMAN	0.0011	−INF	5	5	0	0	0	0
L-xylulose reductase	DCXR_HUMAN	0.0011	−INF	3	4	3	0	0	0
26S protease regulatory subunit 4	PRS4_HUMAN	0.0011	−INF	4	3	3	0	0	0
Ras-related protein Rab-6A	RAB6A_HUMAN	0.0011	−INF	5	5	0	0	0	0
Thioredoxin-like protein 1	TXNL1_HUMAN	0.0011	−INF	3	3	4	0	0	0
Elongation factor 1-alpha 1	EF1A1_HUMAN	0.0011	1.39	47	44	44	70	50	68
Coatomer subunit alpha	COPA_HUMAN	0.0011	2.08	11	7	7	18	15	19
ERO1-like protein alpha	ERO1A_HUMAN	0.0013	0.13	5	4	6	0	2	0
Eukaryotic translation initiation factor 4 gamma 2	IF4G2_HUMAN	0.0018	+INF	0	0	0	3	3	3
N-acetyltransferase 13	NAT13_HUMAN	0.0018	+INF	0	0	0	6	0	3
ATP-dependent RNA helicase DDX3X	DDX3X_HUMAN	0.002	5.33	0	3	0	6	5	5
Transferrin receptor protein 1	TFR1_HUMAN	0.002	5.33	0	0	3	6	5	5
ADP/ATP translocase 1	ADT1_HUMAN	0.0021	−INF	0	0	9	0	0	0
ADP/ATP translocase 3	ADT3_HUMAN	0.0021	−-INF	0	0	9	0	0	0
Rab GDP dissociation inhibitor alpha	GDIA_HUMAN	0.0021	−INF	3	2	4	0	0	0
Glycogen phosphorylase, brain form	PYGB_HUMAN	0.0021	−INF	2	3	4	0	0	0
Splicing factor 3B subunit 1	SF3B1_HUMAN	0.0021	−INF	5	4	0	0	0	0
Inosine-5'-monophosphate dehydrogenase 2	IMDH2_HUMAN	0.0024	0.22	10	0	8	0	0	4
Rho GTPase-activating protein 1	RHG01_HUMAN	0.0029	3.80	0	3	2	11	0	8
Neurosecretory protein VGF	VGF_HUMAN	0.003	0.56	22	27	19	18	16	4
Lactoylglutathione lyase	LGUL_HUMAN	0.0034	0.29	7	8	6	3	3	0
Calumenin	CALU_HUMAN	0.0034	5.00	0	0	3	3	4	8

(*continued on next page*)

Table 3 (*continued*)

Protein name	UniProtKB/Swiss-Prot identifier	*p*-value	T/C ratio	Total spectra					
				C1C	C2C	C3C	T1C	T2C	T3C
14–3-3 protein eta	1433F_HUMAN	0.0036	+INF	0	0	0	0	0	8
Seryl-tRNA synthetase, cytoplasmic	SYSC_HUMAN	0.0036	+INF	0	0	0	4	4	0
Myosin-9	MYH9_HUMAN	0.0037	1.34	63	23	51	81	33	69
Adipocyte plasma membrane-associated protein	APMAP_HUMAN	0.004	0.33	8	6	10	3	3	2
NSFL1 cofactor p47	NSF1C_HUMAN	0.0041	0.15	6	4	3	0	2	0
Keratin, type II cytoskeletal 2 epidermal	K22E_HUMAN	0.0041	0.52	14	20	18	6	10	11
Protein FAM115A	F115A_HUMAN	0.0042	−INF	3	3	2	0	0	0
Inositol-3-phosphate synthase 1	INO1_HUMAN	0.0042	−INF	2	2	4	0	0	0
Inositol 1,4,5-trisphosphate receptor type 1	ITPR1_HUMAN	0.0042	−INF	0	2	6	0	0	0
Prefoldin subunit 3	PFD3_HUMAN	0.0042	−INF	0	5	3	0	0	0
GTP-binding protein SAR1a	SAR1A_HUMAN	0.0042	−INF	4	4	0	0	0	0
Transcription factor A, mitochondrial	TFAM_HUMAN	0.0042	−INF	0	4	4	0	0	0
Zyxin	ZYX_HUMAN	0.0047	2.88	0	6	2	8	7	8
Ran-specific GTPase-activating protein	RANG_HUMAN	0.0053	0.30	7	6	7	0	3	3
Keratin, type I cytoskeletal 14	K1C14_HUMAN	0.0056	0.42	8	10	13	5	0	8
DNA-dependent protein kinase catalytic subunit	PRKDC_HUMAN	0.0063	0.63	36	26	21	28	13	11
Keratin, type I cytoskeletal 9	K1C9_HUMAN	0.0069	0.63	35	16	29	21	11	18
Phospholipase D3	PLD3_HUMAN	0.007	0.17	4	4	4	2	0	0
Far upstream element-binding protein 1	FUBP1_HUMAN	0.007	0.21	5	5	4	0	3	0
Eukaryotic initiation factor 4A-I	IF4A1_HUMAN	0.0073	1.42	26	28	25	38	37	37
Guanine nucleotide-binding protein G(I)/G(S)/G(T) subunit beta-2	GBB2_HUMAN	0.0074	+INF	0	0	0	3	0	4
Lamin-B receptor	LBR_HUMAN	0.0074	+INF	0	0	0	4	0	3
Lysophospholipid acyltransferase 7	MBOA7_HUMAN	0.0074	+INF	0	0	0	4	0	3
Dolichyl-diphosphooligosaccharide–protein glycosyltransferase 48 kDa subunit	OST48_HUMAN	0.0074	+INF	0	0	0	0	4	3
Proteasome subunit beta type-4	PSB4_HUMAN	0.0074	+INF	0	0	0	0	5	2
DnaJ homolog subfamily B member 11	DJB11_HUMAN	0.0083	−INF	3	4	0	0	0	0
Glucosamine 6-phosphate N-acetyltransferase	GNA1_HUMAN	0.0083	−INF	4	0	3	0	0	0
Keratin, type II cytoskeletal 5	K2C5_HUMAN	0.0083	−INF	0	0	7	0	0	0
Nicastrin	NICA_HUMAN	0.0083	−INF	5	2	0	0	0	0
Sorting nexin-3	SNX3_HUMAN	0.0083	−INF	4	3	0	0	0	0
Alanyl-tRNA synthetase, cytoplasmic	SYAC_HUMAN	0.0083	−INF	0	5	2	0	0	0
Drebrin	DREB_HUMAN	0.0085	2.86	0	2	5	9	8	3
C-1-tetrahydrofolate synthase, cytoplasmic	C1TC_HUMAN	0.0095	0.40	8	10	7	0	4	6
Neuromodulin	NEUM_HUMAN	0.01	3.00	3	3	0	6	5	7
Valyl-tRNA synthetase	SYVC_HUMAN	0.01	5.50	0	0	2	6	2	3
Heat shock protein beta-1	HSPB1_HUMAN	0.011	1.68	9	13	9	16	18	18
T-complex protein 1 subunit gamma	TCPG_HUMAN	0.014	0.59	17	13	24	10	11	11
Fermitin family homolog 2	FERM2_HUMAN	0.015	2.17	4	5	3	9	4	13
Adenosine kinase	ADK_HUMAN	0.015	+INF	0	0	0	3	0	3
Cysteine and glycine-rich protein 1	CSRP1_HUMAN	0.015	+INF	0	0	0	3	3	0
Hypoxanthine–guanine phosphoribosyltransferase	HPRT_HUMAN	0.015	+INF	0	0	0	4	0	2
BTB/POZ domain-containing protein KCTD12	KCD12_HUMAN	0.015	+INF	0	0	0	0	3	3
RNA-binding protein 8A	RBM8A_HUMAN	0.015	+INF	0	0	0	3	3	0
39S ribosomal protein L12, mitochondrial	RM12_HUMAN	0.015	+INF	0	0	0	3	0	3
FACT complex subunit SSRP1	SSRP1_HUMAN	0.015	+INF	0	0	0	4	2	0
Transmembrane 9 superfamily member 3	TM9S3_HUMAN	0.015	+INF	0	0	0	3	0	3
Cystathionine beta-synthase	CBS_HUMAN	0.016	−INF	3	0	3	0	0	0
Translation initiation factor eIF-2B subunit alpha	EI2BA_HUMAN	0.016	−INF	0	3	3	0	0	0
Filamin-C	FLNC_HUMAN	0.016	−INF	0	0	6	0	0	0
Eukaryotic translation initiation factor 4E	IF4E_HUMAN	0.016	−INF	0	6	0	0	0	0
Protein ERGIC-53	LMAN1_HUMAN	0.016	−INF	4	0	2	0	0	0
Membrane-associated progesterone receptor component 2	PGRC2_HUMAN	0.016	−INF	4	0	2	0	0	0
Proteolipid protein 2	PLP2_HUMAN	0.016	−INF	0	3	3	0	0	0
Cytochrome b-c1 complex subunit 1, mitochondrial	QCR1_HUMAN	0.016	−INF	3	0	3	0	0	0
Signal peptidase complex subunit 3	SPCS3_HUMAN	0.016	−INF	3	0	3	0	0	0
Tumor protein D54	TPD54_HUMAN	0.016	−INF	0	3	3	0	0	0
Dual specificity protein phosphatase 3	DUS3_HUMAN	0.016	4.00	3	0	0	0	6	6
Exportin-1	XPO1_HUMAN	0.016	4.00	3	0	0	4	5	3

Table 3 (*continued*)

Protein name	UniProtKB/Swiss-Prot identifier	*p*-value	T/C ratio	Total spectra					
				C1C	C2C	C3C	T1C	T2C	T3C
Translin	TSN_HUMAN	0.018	5.00	0	2	0	2	3	5
Tubulin beta-2C chain	TBB2C_HUMAN	0.019	0.79	78	71	67	47	52	72
Peroxiredoxin-2	PRDX2_HUMAN	0.019	3.00	5	0	0	4	7	4
Alpha-centractin	ACTZ_HUMAN	0.021	0.20	3	7	0	2	0	0
PDZ and LIM domain protein 5	PDLI5_HUMAN	0.023	3.25	2	0	2	4	4	5
Calnexin	CALX_HUMAN	0.024	0.59	14	13	17	9	8	9
ATP-dependent RNA helicase A	DHX9_HUMAN	0.027	0.31	3	8	2	0	0	4
Golgin subfamily B member 1	GOGB1_HUMAN	0.027	0.31	5	5	3	2	0	2
Importin-5	IPO5_HUMAN	0.027	0.31	7	3	3	2	2	0
Adenylyl cyclase-associated protein 1	CAP1_HUMAN	0.027	0.64	14	18	23	13	8	14
Thymidine kinase, cytosolic	KITH_HUMAN	0.027	3.67	0	0	3	4	3	4
Heat shock cognate 71 kDa protein	HSP7C_HUMAN	0.029	1.16	85	95	84	103	109	93
Calreticulin	CALR_HUMAN	0.029	1.43	12	13	21	17	28	21
26S proteasome non-ATPase regulatory subunit 11	PSD11_HUMAN	0.029	2.43	3	4	0	8	4	5
Growth factor receptor-bound protein 2	GRB2_HUMAN	0.029	2.80	2	3	0	4	4	6
Cytoplasmic dynein 1 heavy chain 1	DYHC1_HUMAN	0.03	0.84	121	96	113	122	61	95
Acylglycerol kinase, mitochondrial	AGK_HUMAN	0.03	+INF	0	0	0	3	2	0
UPF0468 protein C16orf80	CP080_HUMAN	0.03	+INF	0	0	0	3	2	0
Early endosome antigen 1	EEA1_HUMAN	0.03	+INF	0	0	0	2	0	3
Lon protease homolog, mitochondrial	LONM_HUMAN	0.03	+INF	0	0	0	0	5	0
Reticulon-3	RTN3_HUMAN	0.03	+INF	0	0	0	3	0	2
Poly [ADP-ribose] polymerase 1	PARP1_HUMAN	0.031	1.59	12	8	7	17	10	16
Probable cation-transporting ATPase 13A1	AT131_HUMAN	0.031	4.50	0	2	0	2	4	3
Phosphoribosylformylglycinamidine synthase	PUR4_HUMAN	0.031	4.50	0	2	0	0	6	3
2′,3′-cyclic-nucleotide 3′-phosphodiesterase	CN37_HUMAN	0.033	−INF	0	2	3	0	0	0
Dynactin subunit 1	DCTN1_HUMAN	0.033	−INF	2	3	0	0	0	0
2,4-dienoyl-CoA reductase, mitochondrial	DECR_HUMAN	0.033	−INF	3	0	2	0	0	0
Eukaryotic translation initiation factor 2A	EIF2A_HUMAN	0.033	−INF	0	3	2	0	0	0
Extended synaptotagmin-1	ESYT1_HUMAN	0.033	−INF	2	0	3	0	0	0
Glutathione synthetase	GSHB_HUMAN	0.033	−INF	2	3	0	0	0	0
Lamin-A/C	LMNA_HUMAN	0.033	−INF	2	0	3	0	0	0
Plasminogen activator inhibitor 1 RNA-binding protein	PAIRB_HUMAN	0.033	−INF	0	0	5	0	0	0
Ras-related protein Rab-21	RAB21_HUMAN	0.033	−INF	3	2	0	0	0	0
39S ribosomal protein L9, mitochondrial	RM09_HUMAN	0.033	−INF	0	2	3	0	0	0
TAR DNA-binding protein 43	TADBP_HUMAN	0.033	−INF	2	3	0	0	0	0
Ubiquilin-1	UBQL1_HUMAN	0.033	−INF	0	3	2	0	0	0
Vacuolar protein sorting-associated protein 35	VPS35_HUMAN	0.033	−INF	0	3	2	0	0	0
Xenotropic and polytropic retrovirus receptor 1	XPR1_HUMAN	0.033	−INF	2	0	3	0	0	0
Secretory carrier-associated membrane protein 3	SCAM3_HUMAN	0.034	0.36	5	5	4	0	0	5
Arginyl-tRNA synthetase, cytoplasmic	SYRC_HUMAN	0.034	0.36	6	3	5	2	0	3
Rho-related GTP-binding protein RhoC	RHOC_HUMAN	0.036	3.00	0	4	0	4	3	5
Xaa-Pro aminopeptidase 1	XPP1_HUMAN	0.036	3.00	2	0	2	2	7	3
Interleukin enhancer-binding factor 2	ILF2_HUMAN	0.037	0.54	12	8	8	2	4	9
Tubulin-specific chaperone A	TBCA_HUMAN	0.041	0.55	8	12	9	5	7	4
Ubiquitin-like modifier-activating enzyme 1	UBA1_HUMAN	0.042	0.74	29	36	26	25	23	19
Serine/threonine-protein phosphatase 2A 65-kDa regulatory subunit A alpha isoform	2AAA_HUMAN	0.043	0.40	6	3	6	3	0	3
Elongation factor 2	EF2_HUMAN	0.043	1.16	63	72	68	76	74	86
60S ribosomal protein L9	RL9_HUMAN	0.043	3.33	0	0	3	0	3	7
60S ribosomal protein L8	RL8_HUMAN	0.045	2.60	0	0	5	3	8	2
Kinesin-like protein KIF21A	KI21A_HUMAN	0.046	0.60	12	10	13	6	6	9
Vesicle-associated membrane protein-associated protein B/C	VAPB_HUMAN	0.048	0.47	5	7	7	0	3	6
Importin-7	IPO7_HUMAN	0.048	1.79	4	5	5	11	10	4

increase of total transportin 1 in RanBP1-silenced cells by comparing immunofluorescence signal intensities ($p < 0.001$) (Fig. 4A, B). Similarly, a significant, although lesser, increase of transportin 1 was noticed in TDP-43-silenced cells 96 h after transfection (data not shown).

DISCUSSION

TDP-43 depletion from nuclei of neurons with large cytoplasmic inclusions is one of the hallmark features of ALS and FTLD. To study the effect of TDP-43 depletion/

Table 4. Gene ontology analysis (DAVID) of biological processes of differentially expressed proteins identified in proteomic study. The top 10 categories are presented

Term	Count	%	*p*-value	Genes
RNA processing	32	12.3	3.59E−09	PABPC4, UTP15, DIMT1L, PNN, HNRNPL, SF3B1, IMP3, DDX17, RPL7, RBM8A, TARDBP, SRRM2, ISY1, MAGOHB, RPL11, PABPC1, RBM28, FTSJ3, DHX9, PPP2R1A, SARS, AARS, SF1, PRPF3, ELAVL4, PRPF6, RPS7, EIF4A3, HNRNPH3, KHSRP, DDX54, UTP14A
Intracellular transport	29	11.1	6.89E−06	XPO1, COPA, NUP160, EEA1, CALR, LMAN1, RAE1, RPL11, RANBP1, PAFAH1B1, VPS35, SAR1A, HSPA8, AP2M1, ACTC1, SCAMP3, HSP90AA1, SLC25A6, MYH9, YWHAG, YWHAH, SLC25A13, RPL23, IPO7, NUP205, IPO5, SPTBN1, GNAS, MYBBP1A
Macromolecular complex assembly	28	10.7	2.42E−05	XPO1, TUBB2B, GRB2, HP1BP3, TUBB2C, EIF2A, CALR, HPRT1, TFAM, LONP1, MDN1, TUBA1B, TUBB4, PPP2R1A, HIST1H2BB, HIST1H2BC, HSP90AA1, SF1, DECR1, PRPF6, SOD2, TBCA, IPO7, NUP205, IPO5, HIST1H3A, HSPD1, SEPT9
Macromolecular complex subunit organization	28	10.7	7.45E−05	XPO1, TUBB2B, GRB2, HP1BP3, TUBB2C, EIF2A, CALR, HPRT1, TFAM, LONP1, MDN1, TUBA1B, TUBB4, PPP2R1A, HIST1H2BB, HIST1H2BC, HSP90AA1, SF1, DECR1, PRPF6, SOD2, TBCA, IPO7, NUP205, IPO5, HIST1H3A, HSPD1, SEPT9
Protein localization	28	10.7	0.002154	XPO1, COPA, NUP160, SNX3, CALR, LMAN1, CANX, RPL11, VPS35, RAB6A, POM121C, SAR1A, RAB21, AP2M1, GDI1, NUP153, SCAMP3, LYN, MYH9, FLNB, YWHAG, YWHAH, RPL23, IPO7, NUP205, IPO5, SPTBN1, GNAS
Translation	27	10.3	7.64E−11	RPL18, ABCF1, RPL15, PABPC4, EIF2A, VARS, MRPL12, RPL7, RPL9, RPL8, RPL3, RPL11, MARS, EEF1A1, SARS, AARS, RPL27, MRPL9, EEF2, EIF2B1, RPS7, EIF4G2, EIF4E, RPL23, RARS, EIF4A1, RPS10
Protein transport	27	10.3	5.53E−04	XPO1, COPA, NUP160, SNX3, CALR, LMAN1, CANX, RPL11, VPS35, POM121C, RAB6A, SAR1A, RAB21, AP2M1, GDI1, NUP153, SCAMP3, LYN, MYH9, YWHAG, YWHAH, RPL23, IPO7, NUP205, IPO5, SPTBN1, GNAS
Establishment of protein localization	27	10.3	6.34E−04	XPO1, COPA, NUP160, SNX3, CALR, LMAN1, CANX, RPL11, VPS35, POM121C, RAB6A, SAR1A, RAB21, AP2M1, GDI1, NUP153, SCAMP3, LYN, MYH9, YWHAG, YWHAH, RPL23, IPO7, NUP205, IPO5, SPTBN1, GNAS
Response to organic substance	26	10.0	5.62E−04	HSP90AB1, UQCRC1, VAPB, GRB2, PRKDC, PRDX2, VARS, VGF, HPRT1, ERO1L, DDOST, HSPA8, PPP2R1A, ACTC1, HSP90AA1, LYN, AARS, MAP1B, EIF2B1, NME2, GNB2, TFRC, HSPB1, GNAS, HSPD1, PARP1
Protein complex biogenesis	21	8.0	3.97E−04	XPO1, PPP2R1A, HSP90AA1, TUBB2B, GRB2, TUBB2C, DECR1, HPRT1, CALR, SOD2, TFAM, LONP1, TBCA, IPO7, NUP205, IPO5, HSPD1, TUBA1B, MDN1, TUBB4, SEPT9

sequestration on protein abundance, we performed a proteomic study on TDP-43-silenced human neuroblastoma cells. We identified significant changes in the abundance of 273 candidate-affected proteins. In nuclear fractions 50 proteins were decreased and 56 increased, while in cytoplasmic fractions 94 proteins were decreased and 73 were increased. Most of them are functionally annotated as RNA-processing proteins and proteins involved in intracellular transport, suggesting that these are the most affected processes accompanying TDP-43 depletion. We found and validated that TDP-43 positively regulates protein levels of RanBP1, Dnmt3a and a fragment of CgB. The 40-kDa CgB fragment may correspond to a previously identified fragment starting with SSQEGNPPLE as determined by N-terminal peptide sequencing (Lee and Hook, 2009). Genes coding for all three mentioned proteins have TG stretches in introns and an RNA-binding study showed that TDP-43 binds to these sites (Tollervey et al., 2011). Dnmt3a and CgB transcripts were also identified among the top 25% of enriched RNA targets of TDP-43 in another RNA-binding experiment (Sephton et al., 2011).

The observed changes for RanBP1 and Dnmt3a mirror their reported downregulation on the mRNA level in the same cell line (Tollervey et al., 2011). Downregulation of RanBP1, following TDP-43 knockdown, was also observed in SK-Hep1 cell line (Park et al., 2013). Other significantly changed proteins from our list correlated with reported transcriptomic changes, namely vimentin, Pabpc1, Itpr1 (Polymenidou et al., 2011), hemoglobin subunit alpha (Hba1), histone Hist1h2bc (Yu et al., 2012), neuromodulin (Gap43) (Fiesel et al., 2010) and Eno2 (Park et al., 2013). It is however important to be aware that changes in transcript abundance do not necessarily reflect changes in the level of that protein. The reported changes in transcript abundance after TDP-43 knockdown that did not correlate with the changes that we detected in protein levels and some that even changed in the opposite direction, may reflect various forms of posttranscritptional regulation. The cause of these discrepancies may also be due to the different cell lines and animal models being analyzed.

Evidence of involvement of Dnmt3a in neurodegeneration is suggested by an increase in its mRNA expression level in FTLD brains (Banzhaf-Strathmann et al., 2013). Also, Dnmt3a protein level was shown to be increased in the human ALS motor cortex compared to the control (Chestnut et al., 2011), which does not support the loss of function of TDP-43

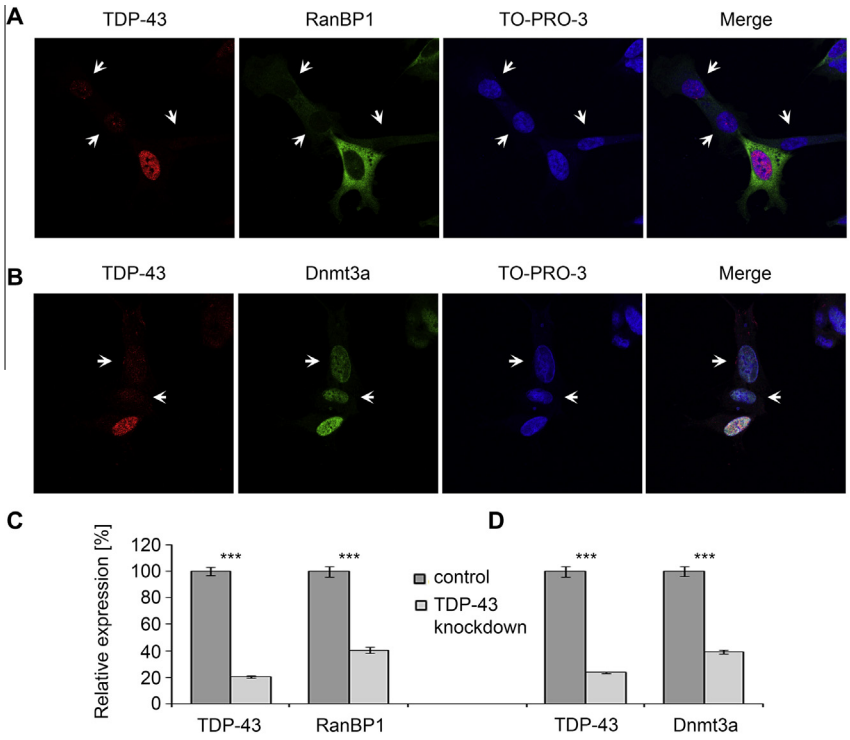

Fig. 3. RanBP1 and Dnmt3a are downregulated when TDP-43 is depleted. SH-SY5Y were transfected with TDP-43 siRNA 1. Immunofluorescence was performed 96 h later. Images show reduction of RanBP1 (A) in cytoplasm and Dnmt3a (B) in nuclei of cells with silenced TDP-43 marked with arrowheads. Immunofluorescence signal intensity was quantified with ImageJ and relative protein expression level was calculated (C, D). Downregulation of RanBP1 and Dnmt3a was statistically significant ($p < 0.001$).

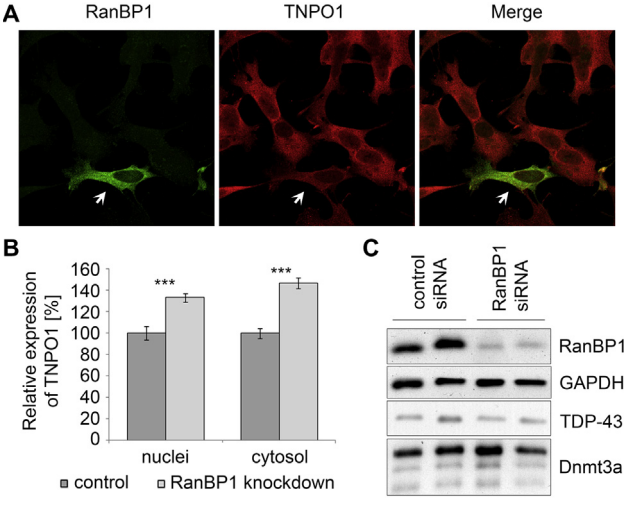

Fig. 4. Increased transportin 1 (TNPO1) level in SH-SY5Y after RanBP1 depletion. SH-SY5Y were transfected with RanBP1 siRNA and immunofluorescence was performed 96 h later. TNPO1 staining is less intensive in untransfected control cell (marked with arrowhead) compared to cells with silenced RanBP1 (A). Quantification of immunofluorescence signal intensity showed that the increase of TNPO1 in RanBP1-silences cells is statistically significant with $p < 0.001$ (B). Panel C shows western blots of SH-SY5Y cell lysates 96 after RanBP1 siRNA transfection. Note that RanBP1 silencing does not affect TDP-43 or Dnmt3a protein levels. GAPDH was used as a loading control.

hypothesis. Chestnut and co-workers (2011) also demonstrated that overexpression of Dnmt3a induces degeneration of neuronal NSC34 cells. On the other hand, mitochondrial Dnmt3a protein level is reduced in the skeletal muscle and spinal cord of transgenic SOD1 mouse models of ALS (Wong et al., 2013).

CgB has also previously been suggested to play a role in neurodegenerative diseases. It accumulates intracellularly in ALS ventral horn motor neurons giving a granular-type of staining (Schrott-Fischer et al., 2009). Its P413L variant is associated with a greater risk for developing ALS and with an earlier age of onset (Gros-Louis et al., 2009). A decreased level of 6251 Da fragment of CgB in cerebrospinal fluid was proposed as a potential biomarker for FTLD (Ruetschi et al., 2005). CgB or its peptide levels are also reduced in the cerebrospinal fluid of patients with multiple sclerosis and schizophrenia (Landen et al., 1999; Mattsson et al., 2007).

TDP-43 depletion may affect intracellular transport through downregulation of RanBP1. The transport of proteins and some other biomolecules through the nuclear envelope with karyopherins is dependent on the RanGTPase system (Melchior et al., 1993), specifically on RanGTP gradient (Izaurralde et al., 1997). In the cytoplasm, RanGTP hydrolyzes to RanGDP upon activation with RanGAP1 (Bischoff et al., 1994). RanBP1 binds directly to RanGTP and stimulates this conversion (Bischoff et al., 1995). Silencing RanBP1 increases overall RanGTP content in cells (Tedeschi et al., 2007) and thus can arrest transport. Furthermore, loss of RanBP1 in mice is embryonically lethal and is associated with microcephaly (Paronett et al., 2014). We provide evidence that RanBP1 is downregulated directly as a result

of TDP-43 depletion. Its mRNA has previously been found to be downregulated in SK-Hep1 cells after TDP-43 knockdown (Park et al., 2013) and in another experiment, binding of TDP-43 in the adjacent intron was shown to promote silencing of exon 5 in RANBP1 transcript (Tollervey et al., 2011), which may have an effect on the observed downregulation of the protein. According to Ensembl, transcripts with included exon 5 may undergo nonsense-mediated decay or may be translated to a protein-lacking N-terminus with a Ran-binding domain, which is responsible for its normal function. We would not be able to detect such a protein with western blot because our antibodies recognize N-terminal amino acids of RanBP1. To date, RanBP1 immunostaining on ALS or FTLD tissue with TDP-43 pathology has not been reported.

We have shown that transportin 1 level is raised in cells as a result of RanBP1 depletion. Nuclear import factors transportin 1 and 2 are responsible for import of fused in sarcoma (FUS), another ALS- and FTLD-involved RNA-binding protein, into the nucleus (Dormann et al., 2010). Transportin 1 colocalizes with FUS aggregates in FTLD with FUS inclusions (FTLD-FUS) (Brelstaff et al., 2011) and ALS with FUS inclusions without FUS mutations (Takeuchi et al., 2013) but not in ALS with FUS mutations (Neumann et al., 2012; Troakes et al., 2013). It does not colocalize with TDP-43 inclusions in FTLD or ALS (Brelstaff et al., 2011; Neumann et al., 2012) but there is variability in nuclear and cytoplasmic staining in ALS with TDP-43 pathology (Troakes et al., 2013). Changes of other karyopherins in ALS and FTLD tissue have also been reported, and furthermore, impairment of the classical import pathway leads to accumulation of TDP-43 in the cytoplasm (Winton et al., 2008; Nishimura et al., 2010), suggesting a feed-forward loop.

Finally, RanBP1 is involved also in axonal transport of proteins. Specifically, it is locally translated in the axon after injury and stimulates the cascade of retrograde injury signaling through interaction with local RanGTP. Blocking of their interaction reduced the level of postlesion neuronal outgrowth (Yudin et al., 2008).

CONCLUSION

Our global proteomic study following depletion of TDP-43 has shown the strongest effect on RNA processing and intracellular transport proteins, giving proteomic support to the accumulating evidence that improper regulation of these proteins and the processes have a role in ALS and FTLD pathology associated with TDP-43 proteinopathy.

Acknowledgments—This work was supported by Slovenian Research Agency [grant numbers J3-2356, J3-4026, J3-5502 and P4-0127], Alzheimer's research UK, the National Institute of Health Research Biomedical Research Center based at Guy's and St Thomas' National Health Service Foundation Trust and King's College London in partnership with King's College Hospital. M. Mayr is a Senior Fellow of the British Heart Foundation.

REFERENCES

Acharya KK, Govind CK, Shore AN, Stoler MH, Reddi PP (2006) Cis-requirement for the maintenance of round spermatid-specific transcription. Dev Biol 295:781–790.

Arai T, Hasegawa M, Akiyama H, Ikeda K, Nonaka T, Mori H, Mann D, Tsuchiya K, Yoshida M, Hashizume Y, Oda T (2006) TDP-43 is a component of ubiquitin-positive tau-negative inclusions in frontotemporal lobar degeneration and amyotrophic lateral sclerosis. Biochem Biophys Res Commun 351:602–611.

Ayala YM, Misteli T, Baralle FE (2008) TDP-43 regulates retinoblastoma protein phosphorylation through the repression of cyclin-dependent kinase 6 expression. Proc Natl Acad Sci U S A 105:3785–3789.

Banzhaf-Strathmann J, Claus R, Mucke O, Rentzsch K, van der Zee J, Engelborghs S, De Deyn PP, Cruts M, van Broeckhoven C, Plass C, Edbauer D (2013) Promoter DNA methylation regulates progranulin expression and is altered in FTLD. Acta Neuropathol Commun 1:16.

Bischoff FR, Klebe C, Kretschmer J, Wittinghofer A, Ponstingl H (1994) RanGAP1 induces GTPase activity of nuclear Ras-related Ran. Proc Natl Acad Sci U S A 91:2587–2591.

Bischoff FR, Krebber H, Smirnova E, Dong W, Ponstingl H (1995) Co-activation of RanGTPase and inhibition of GTP dissociation by Ran-GTP binding protein RanBP1. EMBO J 14:705–715.

Bose JK, Huang CC, Shen CK (2011) Regulation of autophagy by neuropathological protein TDP-43. J Biol Chem 286:44441–44448.

Brelstaff J, Lashley T, Holton JL, Lees AJ, Rossor MN, Bandopadhyay R, Revesz T (2011) Transportin1: a marker of FTLD-FUS. Acta Neuropathol 122:591–600.

Buratti E, Baralle FE (2001) Characterization and functional implications of the RNA binding properties of nuclear factor TDP-43, a novel splicing regulator of CFTR exon 9. J Biol Chem 276:36337–36343.

Buratti E, De Conti L, Stuani C, Romano M, Baralle M, Baralle F (2010) Nuclear factor TDP-43 can affect selected microRNA levels. FEBS J 277:2268–2281.

Chang JC, Hazelett DJ, Stewart JA, Morton DB (2014) Motor neuron expression of the voltage-gated calcium channel cacophony restores locomotion defects in a Drosophila, TDP-43 loss of function model of ALS. Brain Res 1584:39–51.

Chestnut BA, Chang Q, Price A, Lesuisse C, Wong M, Martin LJ (2011) Epigenetic regulation of motor neuron cell death through DNA methylation. J Neurosci 31:16619–16636.

Colombrita C, Zennaro E, Fallini C, Weber M, Sommacal A, Buratti E, Silani V, Ratti A (2009) TDP-43 is recruited to stress granules in conditions of oxidative insult. J Neurochem 111:1051–1061.

Diaper DC, Adachi Y, Lazarou L, Greenstein M, Simoes FA, Di Domenico A, Solomon DA, Lowe S, Alsubaie R, Cheng D, Buckley S, Humphrey DM, Shaw CE, Hirth F (2013a) Drosophila TDP-43 dysfunction in glia and muscle cells cause cytological and behavioural phenotypes that characterize ALS and FTLD. Hum Mol Genet 22:3883–3893.

Diaper DC, Adachi Y, Sutcliffe B, Humphrey DM, Elliott CJ, Stepto A, Ludlow ZN, Vanden Broeck L, Callaerts P, Dermaut B, Al-Chalabi A, Shaw CE, Robinson IM, Hirth F (2013b) Loss and gain of Drosophila TDP-43 impair synaptic efficacy and motor control leading to age-related neurodegeneration by loss-of-function phenotypes. Hum Mol Genet 22:1539–1557.

Dormann D, Rodde R, Edbauer D, Bentmann E, Fischer I, Hruscha A, Than ME, Mackenzie IR, Capell A, Schmid B, Neumann M, Haass C (2010) ALS-associated fused in sarcoma (FUS) mutations disrupt Transportin-mediated nuclear import. EMBO J 29:2841–2857.

Fiesel FC, Voigt A, Weber SS, Van den Haute C, Waldenmaier A, Gorner K, Walter M, Anderson ML, Kern JV, Rasse TM, Schmidt T, Springer W, Kirchner R, Bonin M, Neumann M, Baekelandt V, Alunni-Fabbroni M, Schulz JB, Kahle PJ (2010) Knockdown of transactive response DNA-binding protein (TDP-43) downregulates histone deacetylase 6. EMBO J 29:209–221.

Gendron TF, Petrucelli L (2011) Rodent models of TDP-43 proteinopathy: investigating the mechanisms of TDP-43-mediated neurodegeneration. J Mol Neurosci 45:486–499.
Gitcho MA, Baloh RH, Chakraverty S, Mayo K, Norton JB, Levitch D, Hatanpaa KJ, White 3rd CL, Bigio EH, Caselli R, Baker M, Al-Lozi MT, Morris JC, Pestronk A, Rademakers R, Goate AM, Cairns NJ (2008) TDP-43 A315T mutation in familial motor neuron disease. Ann Neurol 63:535–538.
Gros-Louis F, Andersen PM, Dupre N, Urushitani M, Dion P, Souchon F, D'Amour M, Camu W, Meininger V, Bouchard JP, Rouleau GA, Julien JP (2009) Chromogranin B P413L variant as risk factor and modifier of disease onset for amyotrophic lateral sclerosis. Proc Natl Acad Sci U S A 106:21777–21782.
Hazelett DJ, Chang JC, Lakeland DL, Morton DB (2012) Comparison of parallel high-throughput RNA sequencing between knockout of TDP-43 and its overexpression reveals primarily nonreciprocal and nonoverlapping gene expression changes in the central nervous system of Drosophila. G3 (Bethesda) 2:789–802.
Honda D, Ishigaki S, Iguchi Y, Fujioka Y, Udagawa T, Masuda A, Ohno K, Katsuno M, Sobue G (2014) The ALS/FTLD-related RNA-binding proteins TDP-43 and FUS have common downstream RNA targets in cortical neurons. FEBS Open Bio 4:1–10.
Huang da W, Sherman BT, Lempicki RA (2009a) Bioinformatics enrichment tools: paths toward the comprehensive functional analysis of large gene lists. Nucleic Acids Res 37:1–13.
Huang da W, Sherman BT, Lempicki RA (2009b) Systematic and integrative analysis of large gene lists using DAVID bioinformatics resources. Nat Protoc 4:44–57.
Iguchi Y, Katsuno M, Niwa J, Takagi S, Ishigaki S, Ikenaka K, Kawai K, Watanabe H, Yamanaka K, Takahashi R, Misawa H, Sasaki S, Tanaka F, Sobue G (2013) Loss of TDP-43 causes age-dependent progressive motor neuron degeneration. Brain 136:1371–1382.
Izaurralde E, Kutay U, von Kobbe C, Mattaj IW, Gorlich D (1997) The asymmetric distribution of the constituents of the Ran system is essential for transport into and out of the nucleus. EMBO J 16:6535–6547.
Kabashi E, Lin L, Tradewell ML, Dion PA, Bercier V, Bourgouin P, Rochefort D, Bel Hadj S, Durham HD, Vande Velde C, Rouleau GA, Drapeau P (2010) Gain and loss of function of ALS-related mutations of TARDBP (TDP-43) cause motor deficits in vivo. Hum Mol Genet 19:671–683.
Kabashi E, Valdmanis PN, Dion P, Spiegelman D, McConkey BJ, Vande Velde C, Bouchard JP, Lacomblez L, Pochigaeva K, Salachas F, Pradat PF, Camu W, Meininger V, Dupre N, Rouleau GA (2008) TARDBP mutations in individuals with sporadic and familial amyotrophic lateral sclerosis. Nat Genet 40:572–574.
Keller A, Nesvizhskii AI, Kolker E, Aebersold R (2002) Empirical statistical model to estimate the accuracy of peptide identifications made by MS/MS and database search. Anal Chem 74:5383–5392.
Kraemer BC, Schuck T, Wheeler JM, Robinson LC, Trojanowski JQ, Lee VM, Schellenberg GD (2010) Loss of murine TDP-43 disrupts motor function and plays an essential role in embryogenesis. Acta Neuropathol 119:409–419.
Landen M, Grenfeldt B, Davidsson P, Stridsberg M, Regland B, Gottfries CG, Blennow K (1999) Reduction of chromogranin A and B but not C in the cerebrospinal fluid in subjects with schizophrenia. Eur Neuropsychopharmacol 9:311–315.
Lee JC, Hook V (2009) Proteolytic fragments of chromogranins A and B represent major soluble components of chromaffin granules, illustrated by two-dimensional proteomics with NH(2)-terminal Edman peptide sequencing and MALDI-TOF MS. Biochemistry 48:5254–5262.
Liu YC, Chiang PM, Tsai KJ (2013) Disease animal models of TDP-43 proteinopathy and their pre-clinical applications. Int J Mol Sci 14:20079–20111.
Mattsson N, Ruetschi U, Podust VN, Stridsberg M, Li S, Andersen O, Haghighi S, Blennow K, Zetterberg H (2007) Cerebrospinal fluid concentrations of peptides derived from chromogranin B and secretogranin II are decreased in multiple sclerosis. J Neurochem 103:1932–1939.
Melchior F, Paschal B, Evans J, Gerace L (1993) Inhibition of nuclear protein import by nonhydrolyzable analogues of GTP and identification of the small GTPase Ran/TC4 as an essential transport factor. J Cell Biol 123:1649–1659.
Nesvizhskii AI, Keller A, Kolker E, Aebersold R (2003) A statistical model for identifying proteins by tandem mass spectrometry. Anal Chem 75:4646–4658.
Neumann M, Sampathu DM, Kwong LK, Truax AC, Micsenyi MC, Chou TT, Bruce J, Schuck T, Grossman M, Clark CM, McCluskey LF, Miller BL, Masliah E, Mackenzie IR, Feldman H, Feiden W, Kretzschmar HA, Trojanowski JQ, Lee VM (2006) Ubiquitinated TDP-43 in frontotemporal lobar degeneration and amyotrophic lateral sclerosis. Science 314:130–133.
Neumann M, Valori CF, Ansorge O, Kretzschmar HA, Munoz DG, Kusaka H, Yokota O, Ishihara K, Ang LC, Bilbao JM, Mackenzie IR (2012) Transportin 1 accumulates specifically with FET proteins but no other transportin cargos in FTLD-FUS and is absent in FUS inclusions in ALS with FUS mutations. Acta Neuropathol 124:705–716.
Nishimura AL, Zupunski V, Troakes C, Kathe C, Fratta P, Howell M, Gallo JM, Hortobagyi T, Shaw CE, Rogelj B (2010) Nuclear import impairment causes cytoplasmic trans-activation response DNA-binding protein accumulation and is associated with frontotemporal lobar degeneration. Brain 133:1763–1771.
Ou SH, Wu F, Harrich D, Garcia-Martinez LF, Gaynor RB (1995) Cloning and characterization of a novel cellular protein, TDP-43, that binds to human immunodeficiency virus type 1 TAR DNA sequence motifs. J Virol 69:3584–3596.
Park YY, Kim SB, Han HD, Sohn BH, Kim JH, Liang J, Lu Y, Rodriguez-Aguayo C, Lopez-Berestein G, Mills GB, Sood AK, Lee JS (2013) Tat-activating regulatory DNA-binding protein regulates glycolysis in hepatocellular carcinoma by regulating the platelet isoform of phosphofructokinase through microRNA 520. Hepatology 58:182–191.
Paronett EM, Meechan DW, Karpinski BA, LaMantia AS, Maynard TM (2014) Ranbp1, deleted in DiGeorge/22q11.2 deletion syndrome, is a microcephaly gene that selectively disrupts Layer 2/3 Cortical Projection Neuron Generation. Cereb Cortex.
Polymenidou M, Lagier-Tourenne C, Hutt KR, Huelga SC, Moran J, Liang TY, Ling SC, Sun E, Wancewicz E, Mazur C, Kordasiewicz H, Sedaghat Y, Donohue JP, Shiue L, Bennett CF, Yeo GW, Cleveland DW (2011) Long pre-mRNA depletion and RNA missplicing contribute to neuronal vulnerability from loss of TDP-43. Nat Neurosci 14:459–468.
Ruetschi U, Zetterberg H, Podust VN, Gottfries J, Li S, Hviid Simonsen A, McGuire J, Karlsson M, Rymo L, Davies H, Minthon L, Blennow K (2005) Identification of CSF biomarkers for frontotemporal dementia using SELDI-TOF. Exp Neurol 196:273–281.
Rutherford NJ, Zhang YJ, Baker M, Gass JM, Finch NA, Xu YF, Stewart H, Kelley BJ, Kuntz K, Crook RJ, Sreedharan J, Vance C, Sorenson E, Lippa C, Bigio EH, Geschwind DH, Knopman DS, Mitsumoto H, Petersen RC, Cashman NR, Hutton M, Shaw CE, Boylan KB, Boeve B, Graff-Radford NR, Wszolek ZK, Caselli RJ, Dickson DW, Mackenzie IR, Petrucelli L, Rademakers R (2008) Novel mutations in TARDBP (TDP-43) in patients with familial amyotrophic lateral sclerosis. PLoS Genet 4:e1000193.
Schmid B, Hruscha A, Hogl S, Banzhaf-Strathmann J, Strecker K, van der Zee J, Teucke M, Eimer S, Hegermann J, Kittelmann M, Kremmer E, Cruts M, Solchenberger B, Hasenkamp L, van Bebber F, Van Broeckhoven C, Edbauer D, Lichtenthaler SF, Haass C (2013) Loss of ALS-associated TDP-43 in zebrafish causes muscle degeneration, vascular dysfunction, and reduced motor neuron axon outgrowth. Proc Natl Acad Sci U S A 110:4986–4991.
Schrott-Fischer A, Bitsche M, Humpel C, Walcher C, Maier H, Jellinger K, Rabl W, Glueckert R, Marksteiner J (2009) Chromogranin peptides in amyotrophic lateral sclerosis. Regul Pept 152:13–21.

Sephton CF, Cenik C, Kucukural A, Dammer EB, Cenik B, Han Y, Dewey CM, Roth FP, Herz J, Peng J, Moore MJ, Yu G (2011) Identification of neuronal RNA targets of TDP-43-containing ribonucleoprotein complexes. J Biol Chem 286:1204–1215.

Shevchenko A, Wilm M, Vorm O, Mann M (1996) Mass spectrometric sequencing of proteins silver-stained polyacrylamide gels. Anal Chem 68:850–858.

Shiga A, Ishihara T, Miyashita A, Kuwabara M, Kato T, Watanabe N, Yamahira A, Kondo C, Yokoseki A, Takahashi M, Kuwano R, Kakita A, Nishizawa M, Takahashi H, Onodera O (2012) Alteration of POLDIP3 splicing associated with loss of function of TDP-43 in tissues affected with ALS. PLoS One 7:e43120.

Sreedharan J, Blair IP, Tripathi VB, Hu X, Vance C, Rogelj B, Ackerley S, Durnall JC, Williams KL, Buratti E, Baralle F, de Belleroche J, Mitchell JD, Leigh PN, Al-Chalabi A, Miller CC, Nicholson G, Shaw CE (2008) TDP-43 mutations in familial and sporadic amyotrophic lateral sclerosis. Science 319:1668–1672.

Swarup V, Phaneuf D, Bareil C, Robertson J, Rouleau GA, Kriz J, Julien JP (2011) Pathological hallmarks of amyotrophic lateral sclerosis/frontotemporal lobar degeneration in transgenic mice produced with TDP-43 genomic fragments. Brain 134:2610–2626.

Takeuchi R, Toyoshima Y, Tada M, Shiga A, Tanaka H, Shimohata M, Kimura K, Morita T, Kakita A, Nishizawa M, Takahashi H (2013) Transportin 1 accumulates in FUS inclusions in adult-onset ALS without FUS mutation. Neuropathol Appl Neurobiol 39:580–584.

Tedeschi A, Ciciarello M, Mangiacasale R, Roscioli E, Rensen WM, Lavia P (2007) RANBP1 localizes a subset of mitotic regulatory factors on spindle microtubules and regulates chromosome segregation in human cells. J Cell Sci 120:3748–3761.

Tollervey JR, Curk T, Rogelj B, Briese M, Cereda M, Kayikci M, Konig J, Hortobagyi T, Nishimura AL, Zupunski V, Patani R, Chandran S, Rot G, Zupan B, Shaw CE, Ule J (2011) Characterizing the RNA targets and position-dependent splicing regulation by TDP-43. Nat Neurosci 14:452–458.

Troakes C, Hortobagyi T, Vance C, Al-Sarraj S, Rogelj B, Shaw CE (2013) Transportin 1 colocalization with Fused in Sarcoma (FUS) inclusions is not characteristic for amyotrophic lateral sclerosis-FUS confirming disrupted nuclear import of mutant FUS and distinguishing it from frontotemporal lobar degeneration with FUS inclusions. Neuropathol Appl Neurobiol 39:553–561.

Tsao W, Jeong YH, Lin S, Ling J, Price DL, Chiang PM, Wong PC (2012) Rodent models of TDP-43: recent advances. Brain Res 1462:26–39.

Van Deerlin VM, Leverenz JB, Bekris LM, Bird TD, Yuan W, Elman LB, Clay D, Wood EM, Chen-Plotkin AS, Martinez-Lage M, Steinbart E, McCluskey L, Grossman M, Neumann M, Wu IL, Yang WS, Kalb R, Galasko DR, Montine TJ, Trojanowski JQ, Lee VM, Schellenberg GD, Yu CE (2008) TARDBP mutations in amyotrophic lateral sclerosis with TDP-43 neuropathology: a genetic and histopathological analysis. Lancet Neurol 7:409–416.

Vizcaino JA, Deutsch EW, Wang R, Csordas A, Reisinger F, Rios D, Dianes JA, Sun Z, Farrah T, Bandeira N, Binz PA, Xenarios I, Eisenacher M, Mayer G, Gatto L, Campos A, Chalkley RJ, Kraus HJ, Albar JP, Martinez-Bartolome S, Apweiler R, Omenn GS, Martens L, Jones AR, Hermjakob H (2014) ProteomeXchange provides globally coordinated proteomics data submission and dissemination. Nat Biotechnol 32:223–226.

Volkening K, Leystra-Lantz C, Yang W, Jaffee H, Strong MJ (2009) Tar DNA binding protein of 43 kDa (TDP-43), 14-3-3 proteins and copper/zinc superoxide dismutase (SOD1) interact to modulate NFL mRNA stability. Implications for altered RNA processing in amyotrophic lateral sclerosis (ALS). Brain Res 1305:168–182.

Wegorzewska I, Bell S, Cairns NJ, Miller TM, Baloh RH (2009) TDP-43 mutant transgenic mice develop features of ALS and frontotemporal lobar degeneration. Proc Natl Acad Sci U S A 106:18809–18814.

Wilm M, Shevchenko A, Houthaeve T, Breit S, Schweigerer L, Fotsis T, Mann M (1996) Femtomole sequencing of proteins from polyacrylamide gels by nano-electrospray mass spectrometry. Nature 379:466–469.

Winton MJ, Igaz LM, Wong MM, Kwong LK, Trojanowski JQ, Lee VM (2008) Disturbance of nuclear and cytoplasmic TAR DNA-binding protein (TDP-43) induces disease-like redistribution, sequestration, and aggregate formation. J Biol Chem 283:13302–13309.

Wong M, Gertz B, Chestnut BA, Martin LJ (2013) Mitochondrial DNMT3A and DNA methylation in skeletal muscle and CNS of transgenic mouse models of ALS. Front Cell Neurosci 7:279.

Wu LS, Cheng WC, Shen CK (2012) Targeted depletion of TDP-43 expression in the spinal cord motor neurons leads to the development of amyotrophic lateral sclerosis-like phenotypes in mice. J Biol Chem 287:27335–27344.

Yang C, Wang H, Qiao T, Yang B, Aliaga L, Qiu L, Tan W, Salameh J, McKenna-Yasek DM, Smith T, Peng L, Moore MJ, Brown Jr RH, Cai H, Xu Z (2014) Partial loss of TDP-43 function causes phenotypes of amyotrophic lateral sclerosis. Proc Natl Acad Sci U S A 111:E1121–E1129.

Yin X, Cuello F, Mayr U, Hao Z, Hornshaw M, Ehler E, Avkiran M, Mayr M (2010) Proteomics analysis of the cardiac myofilament subproteome reveals dynamic alterations in phosphatase subunit distribution. Mol Cell Proteomics 9:497–509.

Yokoseki A, Shiga A, Tan CF, Tagawa A, Kaneko H, Koyama A, Eguchi H, Tsujino A, Ikeuchi T, Kakita A, Okamoto K, Nishizawa M, Takahashi H, Onodera O (2008) TDP-43 mutation in familial amyotrophic lateral sclerosis. Ann Neurol 63:538–542.

Yu Z, Fan D, Gui B, Shi L, Xuan C, Shan L, Wang Q, Shang Y, Wang Y (2012) Neurodegeneration-associated TDP-43 interacts with fragile X mental retardation protein (FMRP)/Staufen (STAU1) and regulates SIRT1 expression in neuronal cells. J Biol Chem 287:22560–22572.

Yudin D, Hanz S, Yoo S, Iavnilovitch E, Willis D, Gradus T, Vuppalanchi D, Segal-Ruder Y, Ben-Yaakov K, Hieda M, Yoneda Y, Twiss JL, Fainzilber M (2008) Localized regulation of axonal RanGTPase controls retrograde injury signaling in peripheral nerve. Neuron 59:241–252.

Zhou H, Huang C, Chen H, Wang D, Landel CP, Xia PY, Bowser R, Liu YJ, Xia XG (2010) Transgenic rat model of neurodegeneration caused by mutation in the TDP gene. PLoS Genet 6:e1000887.

(Accepted 24 February 2015)
(Available online 2 March 2015)